Process-informed material model selection

CONDE Mariana[1,a] *, COPPIETERS Sam[2,b] and ANDRADE-CAMPOS António[1,c]

[1]Department of Mechanical Engineering, TEMA - Centre for Mechanical Technology and Automation, LASI - Intelligent Systems Associate Laboratory, University of Aveiro, Campus Universitário de Santiago, 3810-193 Aveiro, Portugal

[2]Department of Materials Engineering, KU Leuven - Ghent Campus, Gebroeders De Smetstraat 1, Ghent, 9000, Belgium

[a]marianaconde@ua.pt, [b]sam.coppieters@kuleuven.be, [c]gilac@ua.pt

Keywords: Material Model Selection, Numerical Simulation, Hole Expansion Test, Analysis of Variance (ANOVA)

Abstract. The efficient development of metal products with high quality usually requires realistic numerical simulations before the manufacturing procedure. The choice of the constitutive model has a considerable influence on the predicted material behavior's description. Several material constitutive models have been proposed to describe different mechanical phenomena. However, its selection is a labored task that requires expertise. This lack of knowledge can lead to errors in the numerical predictions and, consequently, large costs and delays in the manufacturing procedure. To overcome this problem, an automatic material model selection tool is necessary. This work aims to compare the impact of different constitutive models and their features on the simulation of a forming process and develop a rational and systematic strategy for model selection. The approach focuses on the study of a hole expansion test using Abaqus and a statistical analysis of variance (ANOVA). It was possible to establish a ranking for the importance of the types of models that can help with model selection decision-making and efficient parameter calibration for accurate predictions.

Introduction

Nowadays, the aeronautics and automobile industries are in high demand for quality and efficiency. The design and development of products must be precise, with low costs and no delays. Thus, the trend is to virtualize the design of parts, the prototyping, and the manufacturing processes, through numerical simulations. However, in some cases, the lack of knowledge and time to correctly describe the material behavior is observed. This can lead to errors in the numerical simulations and, consequently, large costs and delays in the development and manufacturing processes. When conducting an accurate Finite Element (FE) simulation, an adequate constitutive model and accurately calibrated material parameters are necessary. In the last decades, many models were developed [1-4], implemented in numerical simulations and validated experimentally [1-3]. There are models that account for the microstructural characteristics of the material (i.e. physics-based) but require large computational efforts [1,2]. However, other models describe macroscopically the phenomenological behavior of materials [4-8]. Generally, phenomenological models are an aggregation of formulations that individually try to capture macroscopic phenomena, such as hardening or the elastic-plastic transition. These can be divided into hardening laws [5,8], anisotropic yield functions [3,6,7] and damage models [3,9]. Regarding metals, the prediction of different mechanical phenomena and effects of the material behavior, such as springback, ratcheting, twinning, transformation-induced plasticity (TRIP) and the Bauschinger effect, have been vastly studied in [1,2,10-13]. One of the problems that a simulation software user faces is the selection of the constitutive equations that describe the material behavior. Although there is a vast number of constitutive models and equations, its selection for a specific material

and process usually requires high expertise, an exhaustive investigation and mechanical experimentation. Most of the authors have been comparing different models with experimental data to determine which is more adequate for a specific material and process mainly based on geometrical measurements [1,10-14] and stress-strain curves, or load-displacement curves and yield loci [1,11-15]. Yet, this comparison can be time-consuming since it starts with several mechanical experiments for the identification of different models' parameters, the accurate calibration of the latter and the simulation and validation of the analyzed mechanical process. A flexible and automatic tool or strategy for model selection is lacking in the industry and scientific community.

This work aims at proposing a rational and systematic strategy for the recommendation of constitutive equations that can guide inverse identification methods, such as in [16], with the goal of accurate forming process simulations. The approach involves the numerical simulation of a hole expansion test using the Abaqus FEA software [17] and the analysis of measurements of interest using the analysis of variance (ANOVA) [18]. This statistical methodology was already implemented as a Design of Experiments (DoE) approach to determine the influence of some geometric factors on the springback of sheet metal parts [19-22], but it can be extended to a more general analysis that helps with constitutive model selection.

Methodology

General Methodology. The proposed methodology is based on the analysis of the influence of the material constitutive models used in the numerical simulation of a sheet metal forming process. Some quantities of interest or critical aspects that are present in a metal-forming process were investigated. These quantities can be related to the premature rupture of the blank, its thickness variation, the geometry of the final shape of the sheet or other errors that one can expect in the considered forming process. This data was analyzed using the ANOVA approach which allows us to find a relation between the implemented material constitutive models and the observable quantities of interest in the forming process simulation and, finally, establish an importance ranking for the models. A flowchart describing the general methodology is presented in Fig. 1.
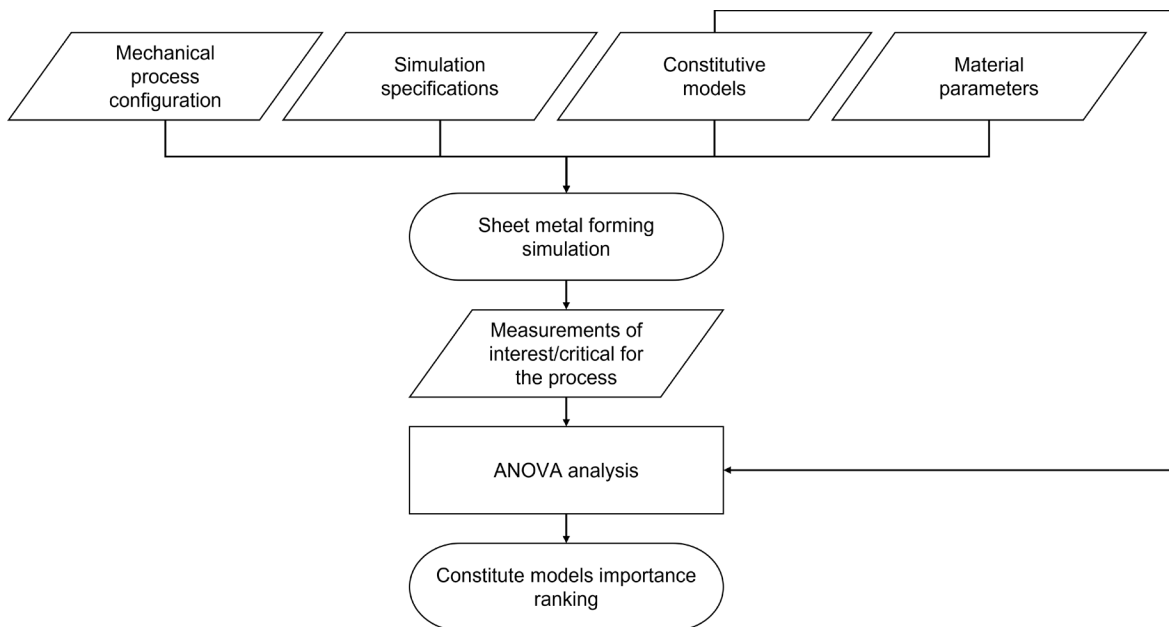
Fig. 1. Flowchart with the general methodology for the material model selection strategy.

ANOVA Strategy. The ANOVA approach is a systematic analysis that allows us to understand the effect of each factor or group (also denoted as independent variables) in the chosen observables

(also denoted as dependent variables) [18]. In this statistical analysis, a hypothesis is tested. The null hypothesis is that there is no difference among the groups' means. The alternative hypothesis is that the averages are not all equal, meaning that at least one group differs significantly from the overall means of the dependent variables. If any of the group means is significantly different from the overall mean, then the **null hypothesis** is rejected. The rejection of the hypothesis can be decided by observing the *p*-value. The *p*-value is defined as the probability of obtaining the observed results, assuming that the null hypothesis is true. It is calculated using the F-statistic and the degrees of freedom for the numerator and denominator. Generally, a *p*-value of 0.05 or lower considers the statistical meaning of the analyzed factor. The smaller the *p*-value is, the more significant the result should be. The F-statistic follows an F-distribution with $(k-1)$ and $(n-k)$ degrees of freddom, where k is the number of groups and n is the total sample size.

Implementation

Hole Expansion Test Simulation Specifications. As a case study, the sheet metal forming process implemented and analyzed in the model selection strategy was the hole expansion test, which was based on [23]. Its configuration and dimensions are depicted in Fig. 2. The simulation was conducted in Abaqus/Standard software [17] using one 3D deformable shell revolution part for the 150 mm diameter blank with 0.8 mm thickness and 35 mm diameter of the hole. Moreover, two 3D analytical rigid shell revolution parts were modeled for the tools (the punch and the die). Concerning the assembly of the parts, the distance between the blank and the die at the beginning of the simulation was 0.4 mm, whereas between the blank and the punch was 0.5 mm.
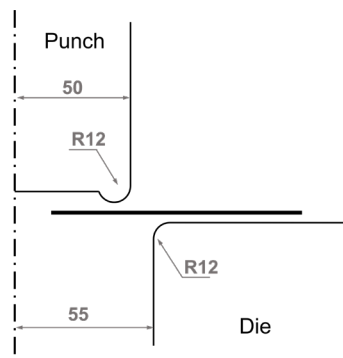
Fig. 2. Hole expansion test configuration (dimensions in mm).

Surface-to-surface contacts were used to define the interactions between the parts with a tangential behavior with penalty and 0.1 friction coefficient and normal behavior of "hard" contact. Besides, contact controls with an automatic stabilization factor of 0.01 were used to avoid convergence issues.

Two static general steps were defined to simulate the non-linear analysis. Initially, two symmetries are established in the blank. In the first step, the punch was moved down with a displacement condition, making sure rupture was not reached independently of the material model and parameters used. Meanwhile, the blank was fixed on the outer edge and the die was also fixed. In the second step, the interactions between the parts were disabled and the vertical displacement of one point of the blank was restricted, to observe the springback behavior of the material.

Regarding the mesh definition, four-node shell elements with reduced integration (S4R) [17] were used in a structured mesh with a total of 6400 elements for the blank, as can be seen in Fig. 3. Furthermore, 9 integration points were calculated along the thickness.
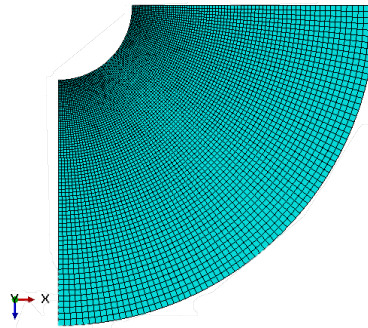
Fig. 3. Mesh of the blank implemented for the hole expansion test.

Material and Constitutive Models Under Analysis. The materials used in the simulations were the DP600 dual-phase steel and the AA3104 aluminum alloy, which behaviors were modelled using the UMMDp (Unified Material Model Driver for Plasticity) from Jancae (Japan Association of Nonlinear CAE) [24]. Concerning the constitutive models under analysis, the Swift hardening law [5], the Voce law [25], the Yld2000-2D for the yield criterion [6] and the Armstrong-Frederick 1966 model (denoted as A-F model) [26] for the kinematic hardening were implemented. The material parameters referring to DP600 [27,28] and AA3104 [29] for the mentioned constitutive models are presented in Table 1. To define the rupture criterion, the Forming Limit Diagram was used [27,30]. Voce's hardening law was fitted to the strain hardening behavior represented by Swift's hardening law.

Table 1. Elastic properties, Swift law, Voce law, Yld2000-2D criterion and Armstrong-Frederick 1966 (A-F model) material parameters for the DP600 steel [27,28] and the AA3104 [29].

DP600								
Elastic properties	E [GPa]				ν			
	210.000				0.300			
Swift law	K [MPa]		ε_0				n	
	979.460		0.00535				0.194	
Voce law	σ_{y0} [MPa]		Q				b	
	815.600		407.922				7.869	
Yld2000-2D criterion	α_1	α_2	α_3	α_4	α_5	α_6	α_7	α_8	a
	1.011	0.964	1.191	0.995	1.010	1.018	0.977	0.935	6.00
A-F model	C [MPa]				γ			
	28896.000				121.000			
AA3104								
Elastic properties	E [GPa]				ν			
	68.950				0.330			
Swift law	K [MPa]		ε_0			n		
	363.128		0.000229			0.0275		
Voce law	σ_{y0} [MPa]		Q				b	
	351.260		62.400				27.205	
Yld2000-2D criterion	α_1	α_2	α_3	α_4	α_5	α_6	α_7	α_8	a
	0.594	1.177	0.818	0.892	0.967	0.627	0.947	1.152	8.00
A-F model	C [MPa]				γ			
	22885.000				400.000			
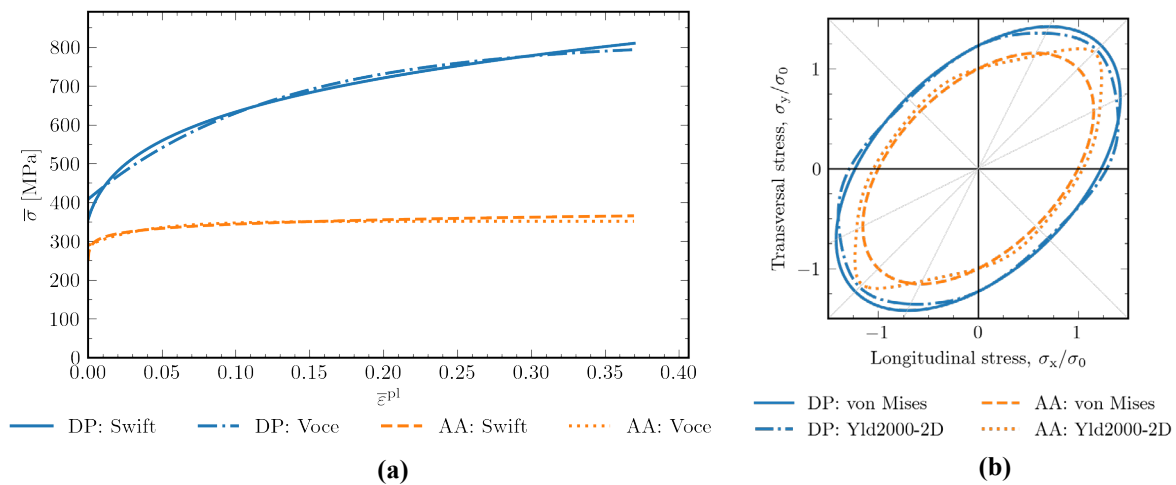
Fig. 4. (a) Plastic strain and stress curves and (b) yield loci for the DP600 and the AA3104 with different material constitutive models.

ANOVA Approach for Model Selection. In this application, the ANOVA approach allows us to establish a relation between each type of constitutive model and its effect in the forming simulation. The type of isotropic, kinematic hardening laws and yield criterion were the independent variables analyzed, whereas the dependent variables were the hole's circularity, the maximum punch force and the springback factor. The hole's circularity is defined as the ratio between the minimum hole's diameter and the maximum hole's diameter, at the end of the simulation. Whereas the springback factor is the ratio between the angle of the deformed sheet before and after the tools' release. Only two levels were analyzed for each factor, being the implementation of the presented models or a simplification of them. In the case of isotropic hardening, the Swift's law or the Voce's law was implemented; for the yield function it was the Yld2000-2D function or the von Mises criterion and for the kinematic hardening it was the A-F model, or no kinematic model was considered. The calculations were made using XLSTAT Cloud add-in for Excel [31].

Results

The hole expansion test simulations using the eight different combinations of the constitutive models presented in Table 2 were conducted for both materials. The obtained outputs of the simulation (dependent variables) are shown in Fig. 5. It can be observed that the hole's circularity is very sensitive to the used yield function (run 1, 3, 5 and 7). For this factor, the AA3104 demonstrates larger sensitivity than the DP600, because the first shows larger variations in the hole's circularity depending on the implemented yield function. Both the maximum punch force and the springback factor are sensitive to the isotropic and kinematic hardening laws used. On contrary, for these dependent variables, the DP600 indicates more sensitivity than the AA3104.

Table 2. Independent variables of the ANOVA approach used for the hole expansion test.

Run	Isotropic hardening law	Yield function	Kinematic hardening law
1	Voce's law	von Mises	Not considered
2	Voce's law	von Mises	A-F model
3	Voce's law	Yld2000-2D	Not considered
4	Voce's law	Yld2000-2D	A-F model
5	Swift's law	von Mises	Not considered
6	Swift's law	von Mises	A-F model
7	Swift's law	Yld2000-2D	Not considered
8	Swift's law	Yld2000-2D	A-F model
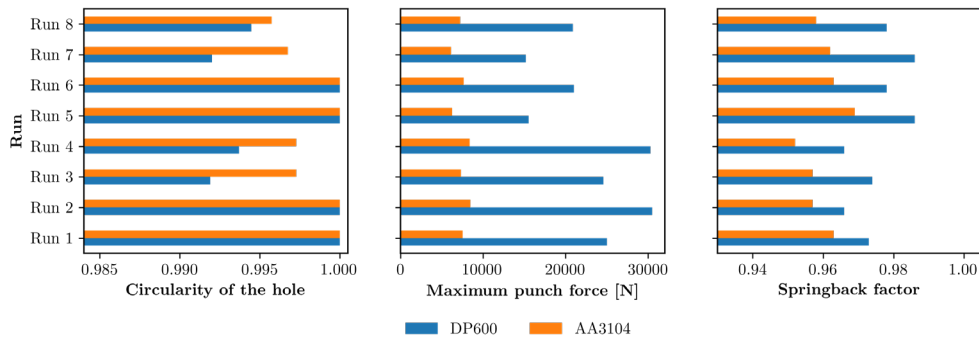
Fig. 5. Hole's circularity, maximum punch force and springback factor obtained from the DP600 and AA3104 simulations using the combination of material models presented in Table 2.

In Table 3, the ANOVA computed results are presented, showing the *p*-values for each factor and dependent variable, the average *p*-value for each factor and the constitutive model's ranking of importance for both materials. As expected, it can be concluded that the yield function is the factor that most influences the hole's circularity, having the lowest *p*-value, independently of the material used. This factor shows a *p*-value lower than 0.05, thus the null hypothesis is rejected. On contrary, and still referring to the hole's circularity, the isotropic and kinematic hardening rules show *p*-values larger than 0.05. Thus, there is no statistical significance of this factor in the hole's circularity. Regarding the maximum punch force, the three factors demonstrate statistical influence on its variation, except for the yield function of AA3104. Both the isotropic and kinematic hardening rules produce a large influence on the maximum punch force, having a very small *p*-value. A similar tendency is observed for the springback factor variation.

Table 3. ANOVA's computed p-values and constitutive model's ranking for the DP600 and AA3104.

Factors	Hole's circularity *p*-value	Maximum punch force *p*-value	Springback factor *p*-value	*p*-value average	Ranking
DP600					
Isotropic hardening law	7.131×10^{-1}	1.078×10^{-8}	2.534×10^{-7}	2.377×10^{-1}	2
Yield function	2.342×10^{-4}	1.436×10^{-2}	9.715×10^{-1}	3.287×10^{-1}	3
Kinematic hardening law	1.282×10^{-1}	8.716×10^{-8}	1.444×10^{-6}	4.274×10^{-2}	1
AA3104					
Isotropic hardening law	2.020×10^{-1}	3.099×10^{-4}	9.909×10^{-6}	6.743×10^{-2}	2
Yield function	6.778×10^{-4}	8.624×10^{-2}	1.037×10^{-5}	2.898×10^{-2}	1
Kinematic hardening law	4.913×10^{-1}	2.881×10^{-4}	1.569×10^{-5}	1.639×10^{-1}	3

Analyzing the overall results for the DP600, the kinematic hardening rule has the lowest computed *p*-value average, meaning that this factor has the largest influence on the average of the considered

dependent variables. Besides, it is also possible to establish a constitutive model's importance ranking for the studied material and mechanical process. The kinematic hardening rule shows the largest influence on the simulation results, followed by the isotropic hardening rule and, finally, the yield function. Indeed, looking at the yield locus of this material (see Fig. 4 (b)), a weak plastic anisotropy can be observed. With this information, simplifying the yield function using von Mises is considered adequate, being not necessary to calibrate a complex yield function to describe the anisotropic phenomena of this material for the considered mechanical process. Moreover, this process deals with continuous bending and unbending of the sheet, which might indicate the relevance of the kinematic hardening rule. Yet, the materials reveal different importance for this model. In Fig. 7, the Schmitt parameter [32] is displayed over time for elements shown in Fig. 6, which are distributed along the radial direction of the sheet metal. This parameter can be used to describe strain path changes and is defined as the cosine of the angle in the strain space between the strain rate tensors during the pre-strain and subsequent strain path. It assumes a value of 1 for monotonic, -1 for reversed and 0 for orthogonal strain paths. Indeed, the three types of strain paths can be observed, especially at the end of the drawing (where the time is equal to 1) and during the tools' release.
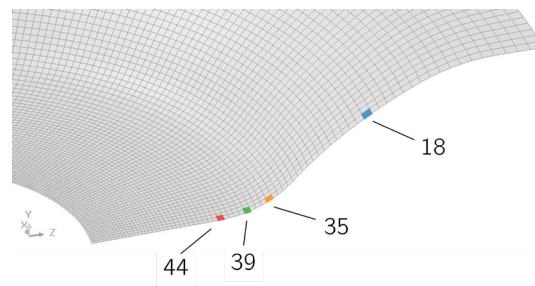
Fig. 6. Location of the elements used to calculate the Schmitt parameter in the deformed blank.
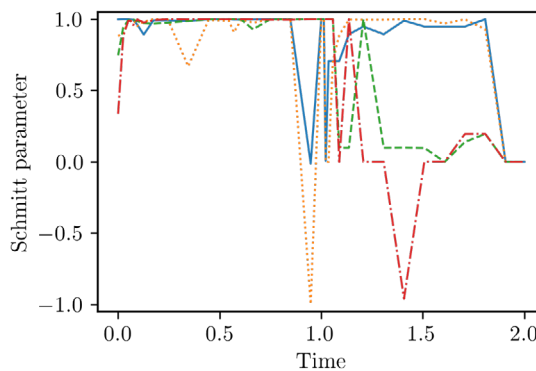
Fig. 7. Schmitt parameter calculated over time in the selected elements for the DP600 (Run 8).

On the contrary, the yield function is the type of model that mainly influences the observables of the AA3104 simulation. This outcome could be expected by looking at the yield locus of the material in Fig. 4 (b). For AA3104, the kinematic hardening rule is the type of model that shows the largest p-value, meaning that it is the factor that hardly influences the analyzed observables. In this case, it is recommended to put efforts into the correct calibration of a complex yield function and discard the kinematic hardening rule. Although the mechanical process considered is the same

as the one used with the DP600 and similar load conditions are imposed, in the case of the AA3104, the ANOVA analysis indicates no significance in the implementation of a kinematic hardening rule to correctly describe the hardening behavior. Fig. 8 displays the Schmitt parameter of some elements along the forming of the AA3104 sheet. Indeed, differences can be detected in the strain paths between the materials. For the AA3104, the instants after the tools' release (time greater than 1.0) show fewer strain path changes, compared with the DP600. This can be explained by the different punch's displacements. The punch's displacement in the DP600 analysis was 16.5 mm whereas in the AA3104 analysis was 12 mm, due to the differences in the rupture of the material.
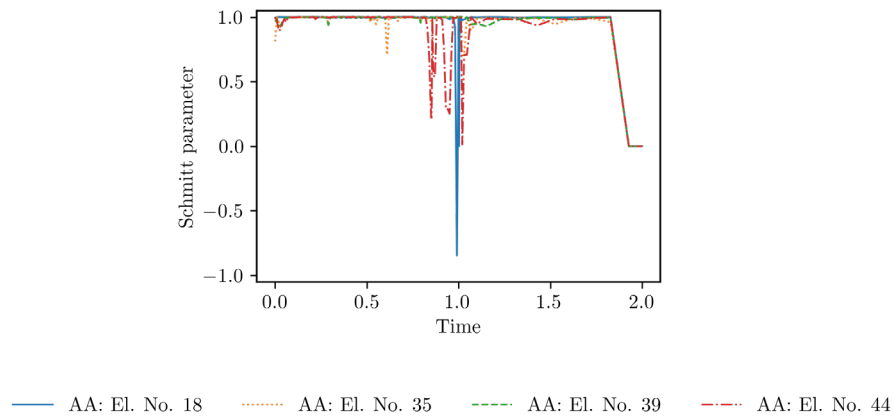
Fig. 8. Schmitt parameter calculated over time in the selected elements for the AA3104 (Run 8).

Summary

In the present work, a process-informed material constitutive model comparison and selection strategy was proposed. The ANOVA methodology was used to establish a relation between the implemented constitutive models in a sheet metal forming simulation and the measures of interest or critical aspects of the process. The outcome of the approach was a constitutive models' importance ranking that indicates the influence of the types of models and mechanical phenomena on the considered forming process. This information is relevant to indicate in which direction should someone focus their efforts concerning material model calibration.

In the study, a hole expansion test simulation was conducted using DP600 dual phase steel and AA3104 aluminum alloy. The ANOVA approach was computed using three factors, the isotropic and kinematic hardening laws, and the yield function. The hole's circularity, the maximum punch force and the resulting springback factor were the dependent variables of the analysis. The differences in the materials' behaviors were clearly observed in the ANOVA results. For the DP600, the most important model was the kinematic hardening, whereas the least important was the yield function. On the contrary, the most important model for the AA3104 was the yield function, whereas the least important was the kinematic hardening rule. These results were expected and confirmed the empirical knowledge by means of a systematic strategy. It must be highlighted that this methodology is material and process-dependent, meaning that for each considered material and mechanical process, a new ANOVA study must be conducted. In the study, the variations in the process conditions, such as friction, temperature and strain rate were not considered and could be interesting to investigate as future works.

Acknowledgements

Disclaimer

The results reflect only the authors' view, and the European Commission is not responsible for any use that may be made of the information it contains.

References

[1] R. Jafari Nedoushan, M. Farzin, D. Banabic, Simulation of hot forming processes: Using cost effective micro-structural constitutive models, Int. J. Mech. Sci. 85 (2014) 196-204. https://doi.org/10.1016/j.ijmecsci.2014.04.026

[2] D.S. Connolly, C.P. Kohar, K. Inal, A novel crystal plasticity model incorporating transformation induced plasticity for a wide range of strain rates and temperatures, Int. J. Plast. 152 (2022) 103188. https://doi.org/10.1016/j.ijplas.2021.103188.

[3] D. Banabic, F. Barlat, O.Cazacu, T. Kuwabara, Advances in anisotropy of plastic behaviour and formability of sheet metals, Int. J. Mater. Form. 13 (2020) 749-787. https://doi.org/10.1007/s12289-020-01580-x

[4] A. Taherizadeh, D.E. Green, J.W. Yoon, Anisotropic hardening model based on non-associated flow rule and combined nonlinear kinematic hardening for sheet materials, AIP Conf Proc 1567 (2013) 496. https://doi.org/10.1063/1.4850020

[5] H.W. Swift, Plastic instability under plane stress, J. Mech. Phys. Solid. 1 (1952) 1-18. https://doi.org/10.1016/0022-5096(52)90002-1

[6] F. Barlat, J.C. Brem, J.W. Yoon, K. Chung, R.E. Dick, D.J. Lege, F. Pourboghrat, S.-H. Choi, E. Chu, Plane stress yield function for aluminum alloy sheets - Part 1: Theory, Int. J. Plast. 19 (2003) 1297-1319. https://doi.org/10.1016/S0749-6419(02)00019-0

[7] D. Banabic, F. Barlat, O. Cazacu, T. Kuwabara, Advances in anisotropy and formability, Int. J. Mater. Form. 3 (2010) 165-189. https://doi.org/10.1007/s12289-010-0992-9.

[8] A.C.S. Reddy, C.B. Reddy, D.V. Paleswar, Review on Different Hardening Models for Computation of Deep Drawing Process Simulation n.d. https://doi.org/10.31224/osf.io/4a28r

[9] D. Banabic, Sheet Metal Forming Processes - Constitutive Modelling and Numerical Simulation, Spinger, 2010. https://doi.org/10.1007/978-3-540-88113-1

[10] S. Ben-Elechi, M. Khelifa, R. Bahloul, Sensitivity of friction coefficients, material constitutive laws and yield functions on the accuracy of springback prediction for an automotive part, Int. J. Mater. Form. 14 (2021) 323-340. https://doi.org/10.1007/s12289-020-01608-2

[11] Y. Hou, J. Min, J. Lin, Z. Liu, J.E. Carsley, B. Thomas, Springback prediction of sheet metals using improved material models, Procedia Eng. 207 (2017) 173-178. https://doi.org/10.1016/j.proeng.2017.10.757

[12] J. Lin, Y. Hou, J. Min, Effect of constitutive model on springback prediction of MP980 and AA6022-T4, Int. J. Mater. Form. 13 (2020) 1-13. https://doi.org/10.1007/s12289-018-01468-x

[13] K. Chatziioannou, Y. Huang, S.A. Karamanos, Simulation of Cyclic Loading on Pipe Elbows Using Advanced Plane-Stress Elastoplasticity Models, J. Press. Vessel. Technol. 143 (2021) 021501-10. https://doi.org/10.1115/1.4047876

[14] V. Prakash, D.R. Kumar, A. Horn, H. Hagenah, M. Merklein, Modeling material behavior of AA5083 aluminum alloy sheet using biaxial tensile tests and its application in numerical simulation of deep drawing, Int. J. Adv. Manuf. Technol. 106 (2020) 1133-1148. https://doi.org/10.1007%2Fs00170-019-04587-0

[15] Z. Tuo, Z. Yue, X. Zhuang, X. Min, H. Badreddine, L. Qiu, Comparison of two uncoupled ductile damage initiation models applied to DP900 steel sheet under various loading paths, Int. J. Damage Mech. 30 (2021) 25-45. https://doi.org/10.1177/1056789520945002

[16] M. Conde, Y. Zhang, J. Henriques, S. Coppieters, A. Andrade-Campos, Design and validation of a heterogeneous interior notched specimen for inverse material parameter identification, Finite Elem. Anal. Des. 214 (2023) 103866. https://doi.org/10.1016/j.finel.2022.103866

[17] Dassault Systèmes. Abaqus 6.14 Online Documentation 2014.

[18] H. Scheffe, The analysis of variance, Vol. 72, John Wiley & Sons, 1999.

[19] P. Teixeira, A. Andrade-Campos, A.D. Santos, F.M.A. Pires, J.M.A. César de Sá, Optimization strategies for springback compensation in sheet metal forming. First ECCOMAS Young Investig, Conf., Aveiro, Portugal, 2012, p. 24-27. https://doi.org/10.1016/B978-0-85709-481-0.00003-3

[20] A. Maia, E. Ferreira, M.C. Oliveira, L.F. Menezes, A. Andrade-Campos, Numerical optimization strategies for springback compensation in sheet metal forming, Comput. Meth. Prod. Eng. Res. Dev. (2017) 51-82. https://doi.org/10.1016/B978-0-85709-481-0.00003-3

[21] H. Naceur, Y.Q. Guo, S. Ben-Elechi, Response surface methodology for design of sheet forming parameters to control springback effects, Comput. Struct. 84 (2006) 1651-1663. https://doi.org/10.1016/j.compstruc.2006.04.005

[22] S. Zhang, L. Léotoing, D. Guines, S. Thuillier, Potential of the Cross Biaxial Test for Anisotropy Characterization Based on Heterogeneous Strain Field, Exp. Mech. 55 (2015) 817-835. https://doi.org/10.1007/s11340-014-9983-y

[23] J. Ha, S. Coppieters, Y.P. Korkolis, International Journal of Mechanical Sciences On the expansion of a circular hole in an orthotropic elastoplastic thin sheet, Int. J. Mech. Sci. 182 (2020) 105706. https://doi.org/10.1016/j.ijmecsci.2020.105706

[24] H. Takizawa, T. Kuwabara, K. Oide, J. Yoshida, Development of the subroutine library "UMMDp" for anisotropic yield functions commonly applicable to commercial FEM codes, J. Phys. Conf. Ser. 734 (2016). https://doi.org/10.1088/1742-6596/734/3/032028

[25] E. Voce, The Relationship between Stress and Strain for Homogeneous Deformation, J. Inst. Met. (1948) 537-562.

[26] P.J. Armstrong, C.O. Frederick, A Mathematical Representation of the Multi Axial Bauschinger Effect, Mater. High Temp. 24 (2007) 1-26. https://doi.org/10.1179/096034007X207589

[27] F. Ozturk, S. Toros, S. Kilic, Effects of anisotropic yield functions on prediction of forming limit diagrams of DP600 advanced high strength steel, Procedia Eng. 81 (2014) 760-765. https://doi.org/10.1016/j.proeng.2014.10.073

[28] J. Fu, F. Barlat, J. Kim, F. Pierron, Identification of nonlinear kinematic hardening constitutive model parameters using the virtual fields method for advanced high strength steels, Int. J. Solid. Struct. 102-103 (2016) 30-43. https://doi.org/https://doi.org/10.1016/j.ijsolstr.2016.10.020

[29] M. Iadicola, Data for Numisheet 2020 uniaxial tensile and tension/compression tests, Natl. Inst. Stand. Technol., 2020. https://doi.org/10.18434/M32202

[30] S.M. Mirfalah-Nasiri, A. Basti, R. Hashemi Forming limit curves analysis of aluminum alloy considering the through-thickness normal stress, anisotropic yield functions and strain rate, Int. J. Mech. Sci. 117 (2016) 93-101. https://doi.org/10.1016/j.ijmecsci.2016.08.011

[31] Addinsoft. XLSTAT n.d. https://www.xlstat.com/en/ (accessed November 21, 2022).

[32] J.H. Schmitt, E. Aernoudt, B. Baudelet, Yield loci for polycrystalline metals without texture, Mater. Sci. Eng. 75 (1985) 13-20. https://doi.org/https://doi.org/10.1016/0025-5416(85)90173-9